Yamanashi Med. J. 13(2), 53 ~ 63, 1998

Experimental Pacemaker Disease Model in Mouse Intestine: Impairment of Interstitial Cells of Cajal by an Antagonistic Antibody for *c-kit*

Ichiro TAKAYAMA, Morio TAKEDA, Shinichi OHNO[1)], and Masayuki A. FUJINO
Departments of Internal Medicine and [1)]Anatomy, Yamanashi Medical University, 1110 Shimokato, Tamaho, Yamanashi 409-3898, Japan

Abstract: An antagonistic antibody, ACK2, for *c-kit* receptor tyrosine kinase was injected into newborn BALB/c mice to block *c-kit* expression. The experimental mice, which were inhibited against the expression of *c-kit* by the ACK2 injection, presented severe paralytic ileus. On the 12th day from birth, normal control mice presented *c-kit* immunoreaction spreading between longitudinal and circular smooth muscle layers of the duodenum, although such immunoreaction did not exist in the myenteric ganglions. That is, the distribution of ACK2-immunoreaction was identical to the localization of the interstitial cells of Cajal (ICC) in the region of the myenteric plexus. In addition, immunoreactions for neuropeptides such as Substance P or vasoactive intestinal peptide presented no remarkable differences between the control and the experimental mice. Electron microscopic examination confirmed ultrastructural impairment of ICC in experimental mice. In comparison with the ICC of control mice, the ICC in the experimental mice dramatically decreased in number and presented an altered ultrastructure with insufficient development of organelles such as mitochondria and Golgi apparatus. Such changes in ICC might be related to the dysmotility of the gut in experimental mice. The *c-kit* expression in newborn mice could be essential for the development of ICC networks or the non-neural intestinal pacemaker system.

Key words: Intestinal pacemaker, Interstitial cells of Cajal, *c-kit*, Special smooth muscle, Mouse.

INTRODUCTION

The *c-kit* is a proto-oncogene, which encodes receptor tyrosine kinase, and is identical with the dominant white spotting (*W*) locus[1-4]. Mice with *W*-mutation are reported to present retardation of developmental specialization in cell lineages of melanocytes, germ cells and haematopoietic cells[5], while the *c-kit* is also expressed in some cells which are phenotypically normal in *W*-mutant mice[6-8]. Nishikawa *et al.* established a monoclonal antibody (referred to as ACK2) for *c-kit* receptor tyrosine kinase, which has an antagonistic effect for *c-kit* receptor tyrosine kinase[9]. Since that time, the ACK2 has been used for revealing specific roles of *c-kit* expression in cell lineages of leukoblasts and melanoblasts[9-10]. Recently, it was discovered by chance that ACK2 injection into newborn BALB/c mice induced serious malnutrition and abdominal swelling, due to the gross dilatation of the gastrointestinal tract[11-12]. However, physiological findings, such as stenosis and obstruction, were never reported in the alimentary tract of the experimental mice. In the present study, we examined a defect of the non-neural components in the intestinal walls of experimental mice, which is considered to be a serious illness, using both immunocytochemistry and electron microscopy. We also discuss the pathological roles of the morphological changes detected in experimental mice.

Received February 10, 1998
Accepted March 3, 1998

MATERIALS AND METHODS

The present study was performed in accordance with the guidelines governing animal experiments, Yamanashi Medical University. Newborn BALB/c mice were obtained from pregnant BALB/c mice, which had been purchased from Japan SLC Inc. (Shizuoka, Japan). An antibody ACK2 for *c-kit* receptor tyrosine kinase established by Nishikawa *et al.*[9] was used in the present study. As described elsewhere[9], ACK2 is a monoclonal antibody of IgG2b class. The experimental mice, whose *c-kit* receptor activity was antagonized by ACK2 injection, were prepared as follows. The 200 μg ACK2 was intraperitoneally injected into the mice every other day from their birth to day 8; thus 5 injections and 1,000 μg of ACK2 in total. Normal control mice were established using injections of normal mouse immunoglobulin of the same class in a similar manner. Body weights of the mice were measured everyday from day 0 to day 10. Histopathological examinations of their duodenum were performed on day 12. Table 1 describes the numbers of control and experimental mice for each preparation.

For immunohistochemical examination for the *c-kit* receptor, both groups were anaesthetized with sodium pentobarbital (400 μg/g), and duodenum segments were immediately dissected. The segments were frozen with liquid nitrogen and cut into sections of 10 μm in a cryostat machine (Coldtome, Sakura, Tokyo). The sections were fixed with acetone at 4 °C for 10 min. They were then rinsed in 0.1 M phosphate buffered saline (PBS), and incubated with ACK2 antibody at a dilution of 1:1,000 at 4 °C for 12 hr. Immunoreactions of ACK2 were visualized by the routine streptavidin-biotin-peroxidase technique.

Zinc-iodide-osmium (ZIO) staining was applied for light microscopic observation[13-14]. Freshly dissected segments of the duodenum were washed in 0.1 M PBS, and placed for fixing and staining in a filtered mixture solution of zinc, iodide and osmium, at 20 °C for 12 hr. Both mucosa and submucosal layers of the specimens were mechanically stripped, and whole mount preparations of the muscle layer alone were established. These were examined under a light microscope.

For immunohistochemical examinations for Substance P and vasoactive intestinal peptide (VIP), duodenal segments were flattened and fixed in Bouin's fixative at 20 °C for 2 hr. They were then rinsed in PBS, and treated with 0.3 % Triton-X 100 in PBS at 4 °C for 24 hr. Treated specimens were incubated with anti-Substance P antibody or anti-VIP antibody, which were established and donated by Prof. N. Yanaihara of Shizuoka Prefectural University, at dilutions of 1:1,000, at 4 °C for 24 hr. These immunoreactions were also visualized by an avidin-biotin-peroxidase technique, as described in a previous paragraph, and whole mount preparations of the muscle layer were established.

For electron microscopy, anaesthetized mice were perfused via the left ventricle with 2 % glu-

Table 1. Numbers of control and experimental mice

	Total	TEM	ZIO	NP	ACK
Control mice	10	3	2	2	3
Experimental mics	9	3	2	2	2

TEM; transmission electron microscopy, ZIO; ZIO staining,
NP; immunostaining for neuropeptides, ACK; immunostaining for ACK2

taraldehyde (GA) in 0.1 M PBS. Then, duodenal segments were dissected, and additionally immersed with 2 % GA in 0.1M PBS, at 4 °C for 12 hr. After prefixation, they were post-fixed in 2 % osmium tetroxide for 2 hr. They were then dehydrated in a graded series of ethanol and routinely embedded in Epok 812. Thick sections stained with toluidine blue (TB) were examined under a light microscope. Ultrathin sections were doubly-stained with uranyl acetate and lead citrate, and examined by Hitachi H-600 electron microscope.

Results

The mean body weight of experimental mice was significantly lower than those of the controls (Fig. 1a). These experimental mice had serious malnutrition and abdominal protrusion on day 12, as shown in Figure 1b-c. However, ascites or tumours did not exist in the peritoneal cavity. Dilated intestinal tracts were filled with bile-coloured contents, and obstruction of the gut was not observed. In contrast, the intestinal tracts of the control mice had white contents without dilatation. Figure 1d-e shows the length and thickness of the intestine, which were measured as in Figure 1b-c. The whole gut of the experimental mice was relatively heavy with congested contents, although their body weight was lower than that of the controls. Therefore, as shown in Table 2, the intestine weight/body weight ratios were dramatically increased in the experimental mice. Figure 2a-c shows immunohistochemistry for *c-kit* by ACK2 antibody. In the duodenum of the control mice, ACK2-immunoreactions were localized between the longitudinal muscle layer and the circular layer (Fig. 2a-c). However, no immunoreaction for *c-kit* was observed in the myenteric ganglions (Fig. 2a). In contrast, the experimental mice

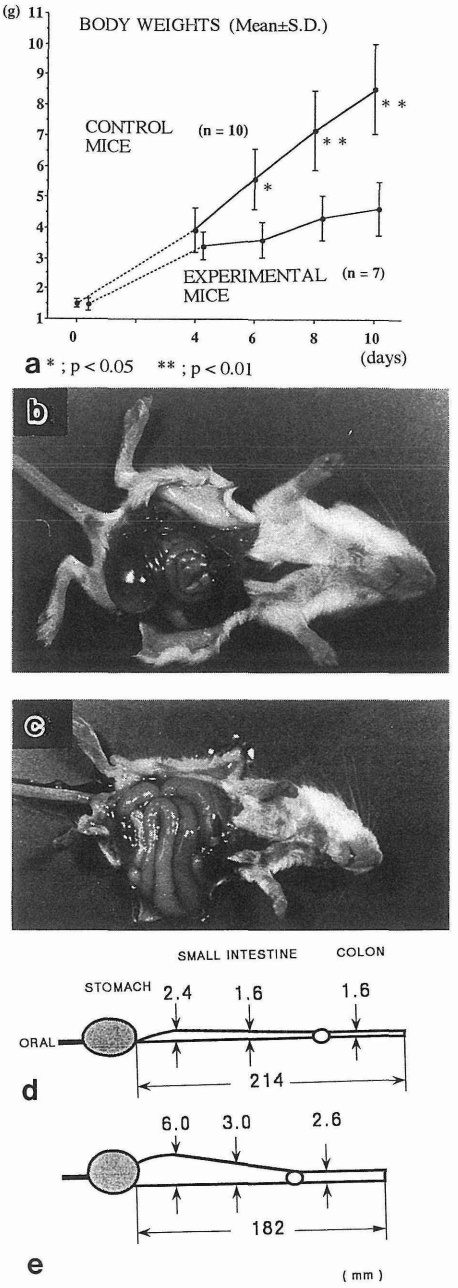

Figure 1. (a) Time-dependent changes of body weights of control and experimental mice. (b) and (c) Gross findings of control (b) and experimental (c) mice by laparotomy. (d) and (e) Schematic representation of the gastrointestinal tract of the control (d) and experimental (e) mice. Note gross intestinal dilatation in the experimental mice.

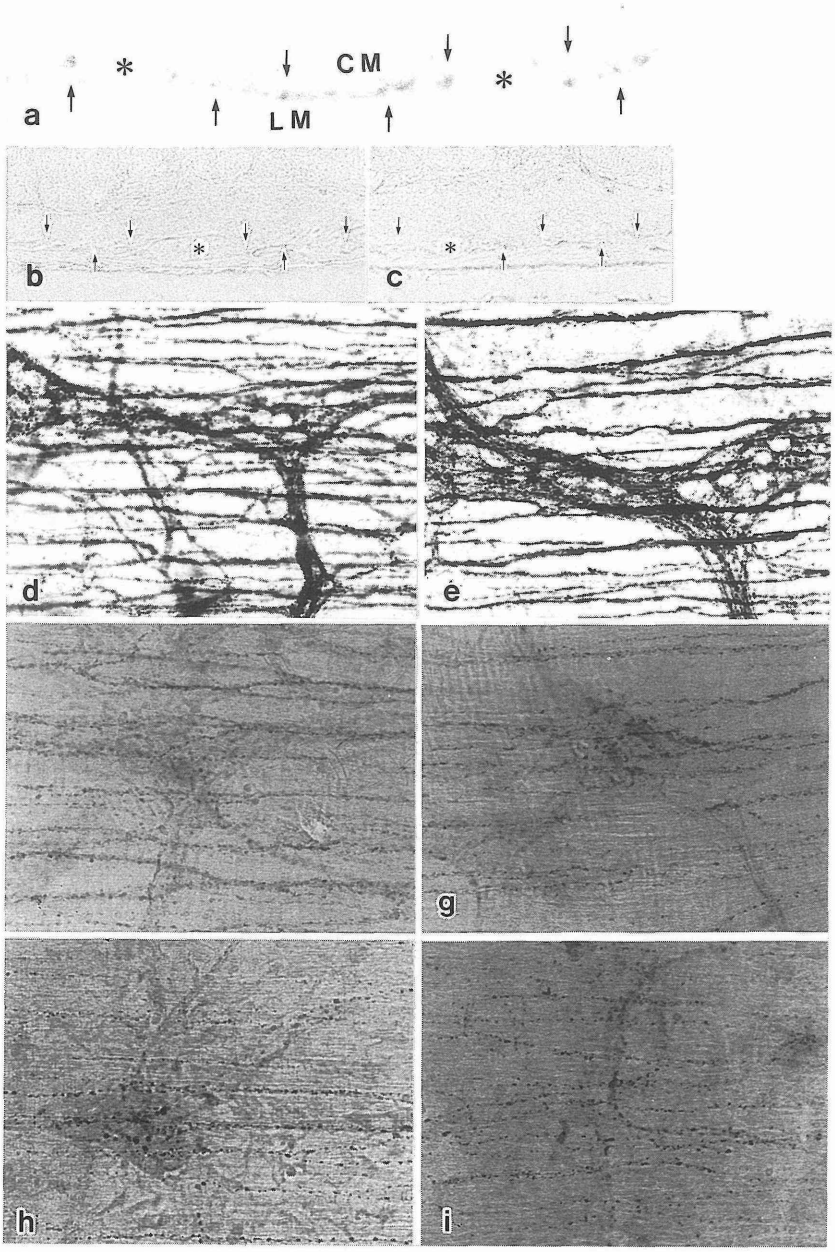

Figure 2. Light micrographs of immunohistochemistry of ACK2. (a) A control mouse. Positive immunoreactions (arrows) are seen between outer longitudinal muscle layer (LM) and inner circular muscle layer (CM). However, myenteric ganglions (asterisks) exhibit no immunoreactions. Magnification; × 780. (b) An experimental mouse. No immunoreactions are observed. Arrows; boundary region. Asterisk; myenteric ganglion. Magnification; × 330. (c) Immunocontrol of a control mouse. No remarkable positive reactions are observed. Arrows; boundary region. Asterisk; myenteric ganglion. Magnification; × 330. (d) and (e) Light micrographs of whole-mount intramural plexuses by ZIO staining method. (d) A control mouse. (e) An experimental mouse. Magnification; × 590. (f)-(i) Light micrographs of immunohistochemistry for neuropeptides, substance P (f,g) or vasoactive intestinal peptide (h,i). (f) and (h) A control mouse. (g) and (i) An experimental mouse. Magnification; × 590.

Table 2. Intestinal weight/body weight ratio in control or experimentl mice on day 12

		Intestinal weight* (g)	Body weight (g)	Ratio (%)
Control mice	case 1	0.65	8.75	7.5
	case 2	0.72	8.90	8.1
Experimental mice	case 1	1.13	4.82	23.5
	case 2	1.30	5.02	25.8

*Intestinal weight includes its contents.

showed no immunoreaction for *c-kit* in the duodenal wall (Fig. 2b), being similar to immunocontrol (Fig. 2c). Network architectures of intramural plexuses in the duodenal wall were revealed on the whole mount preparations by the ZIO method (Fig. 2d-e). No structural changes were observed in the duodenal wall of the experimental mice (Fig. 2e), in comparison with the control mice (Fig. 2d). Figure 2f-i shows the immunoreactions for substance P antibody and VIP in the duodenal wall. Both immunoreactions presented no significant differences between the two groups.

Light micrographs obtained from thick sections of the duodenum revealed several cells characterized with darkly stained cytoplasm that were distributed in regions of the myenteric plexus of the control mice (Fig. 3a). They had long processes and flat nuclei. Most cellular processes were spreading horizontally in boundary regions between the longitudinal muscle layer and the circular layer, although they were not observed in the myenteric ganglions. In contrast, these specific cells were hardly ever found in similar regions of the experimental mice (Fig. 3b). A few cells with relatively dark cytoplasm were observed in the boundary region, though the population was obviously decreased, in comparison with the control mice. Figure 3c shows the ultrastructure of the duodenum in the control mice. Corresponding to the darkly stained cells, some interstitial cells of Cajal (ICC) were detected between the longitudinal muscle layer and the circular layer. These were morphologically similar to fibroblasts and exhibited elongated nuclei, a developed Golgi apparatus, elongated mitochondria and relatively electron-dense cytoplasm (Fig. 3c). In contrast, such cells were hardly ever found in the region of the myenteric plexus in the experimental mice (Fig. 3d). A few cells with thin and short processes were observed in the same boundary region, corresponding to the cells with relatively dark cytoplasm, as shown by light microscopy (Fig. 3b). Such cells, however, were seen much less than ICC in the control mice, and only thin processes were detected in the region of the myenteric plexus. Our electron microscopic examination also revealed no ultrastructural changes of neurons, enteroglial cells and smooth muscle cells.

Finally, we examined the innermost circular muscle layer (Fig. 4). In thick sections of the control mice, a special smooth muscle (SSM) layer, localized in the innermost circular muscle layer, was recognized as being lining cells which were stained with TB (Fig. 4a, inset). The regions between the inner circular muscle layer and the outer one contained cells which were stained darker with TB. Although these cells had flat nuclei, they were smaller than the cells in the region of the myenteric plexus. In the experimental mice, the innermost circular muscle layer was not stained darkly with TB (Fig. 4b, inset). Moreover, darkly stained cells between the inner circular muscle layer and the outer

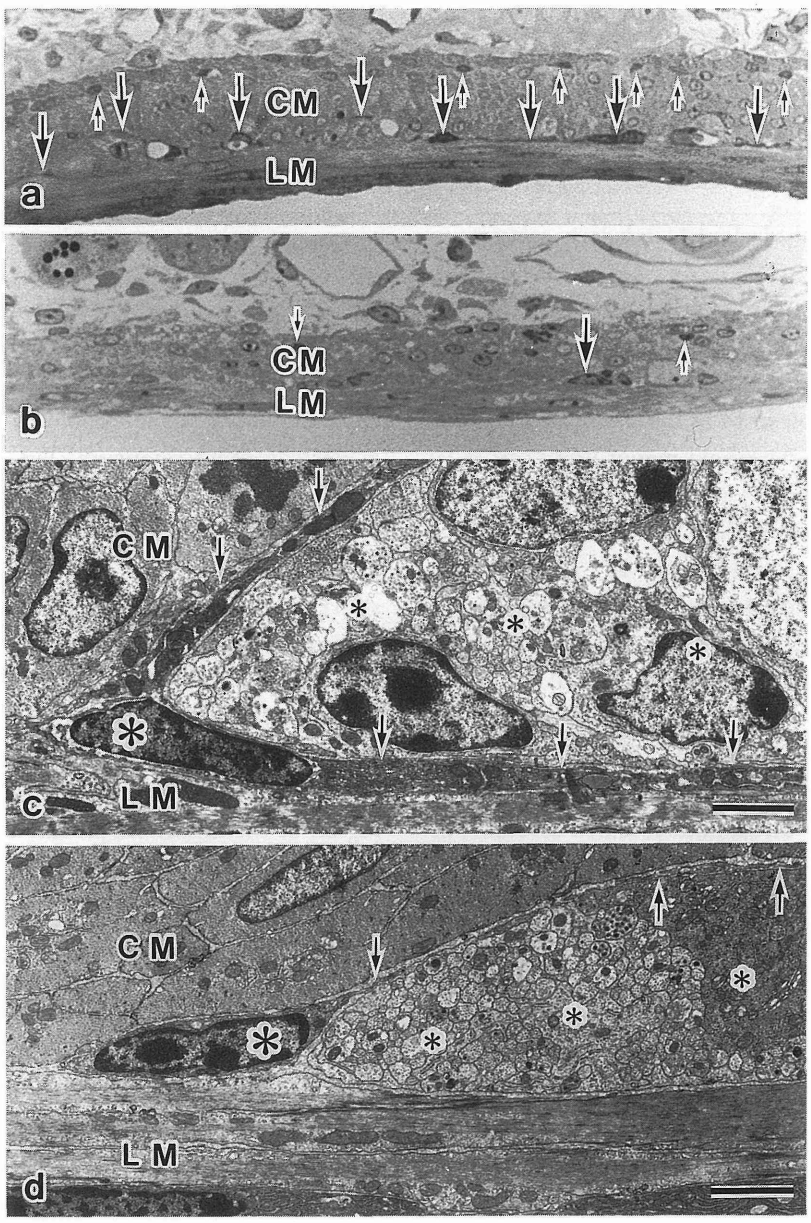

Figure 3. Thick sections of mouse duodenum. (a) In a control mouse, several cells (arrows) with dark nuclei and cytoplasm are localized between longitudinal muscle layer (LM) and circular muscle layer (CM), and also between the inner circular muscle layer and outer circular muscle layer (small arrows). The inner circular muscle layer appears relatively dark. Magnification; × 1,000 (b) In an experimental mouse, a few cells with dark nuclei are seen in both regions (large arrows and small arrows). There is an incomplete inner circular muscle layer. Magnification; × 1,000. (c) and (d) Electron micrographs of boundary regions between the longitudinal muscle layer (LM) and the circular muscle layer (CM). (c) A control mouse. An ICC (large asterisk) has long cytoplasmic processes (arrows) which often surround a myenteric ganglion (small asterisks). (d) In an experimental mouse, ICC-like cells almost disappear. Magnification; × 5,400. Bar; 2 μm.

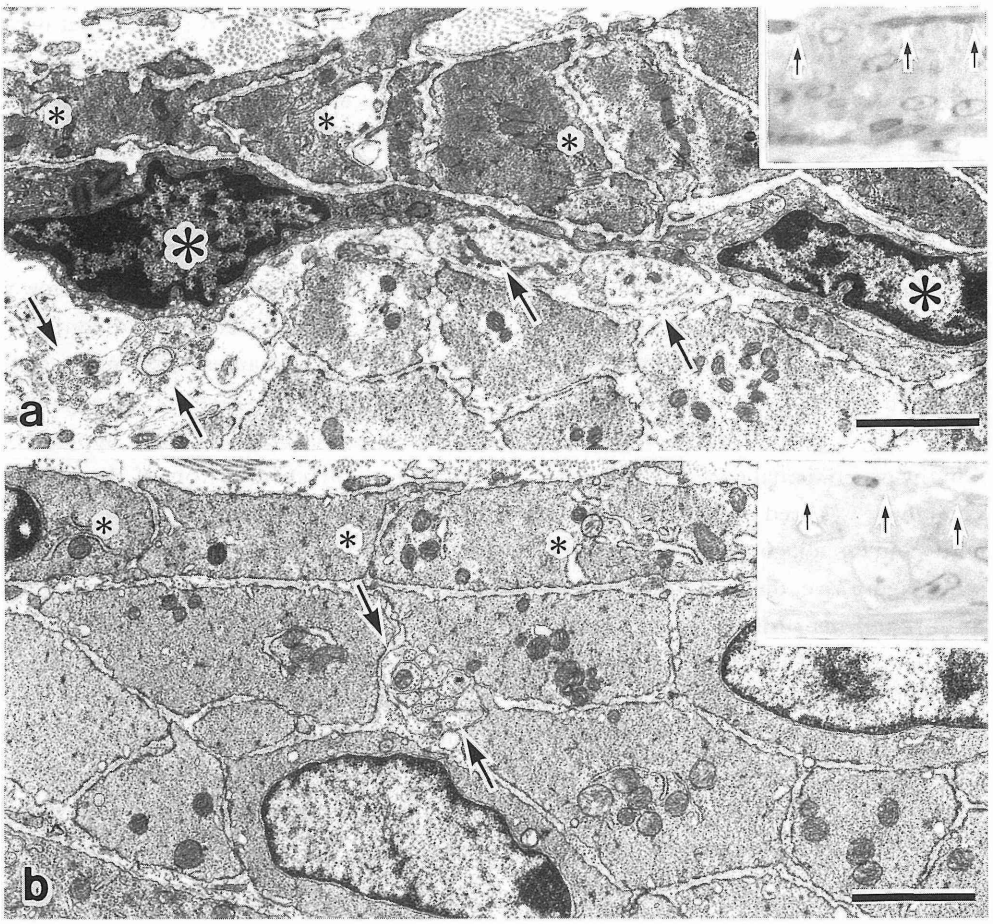

Figure 4. Light or electron micrographs of the innermost layer of the circular muscle layer. (a) A control mouse. Special smooth muscle (small asterisks) layer and ICC (asterisks) are seen in the submucosal border of the circular muscle layer. Arrows; nerve fiber profiles of the deep muscular plexus containing various synaptic vesicles. (b) An experimental mouse. Both SSM and ICC are equivocal. Magnification; × 8,400. Bar; 2 μm.

one were remarkably decreased in comparison to those of the control mice. Electron microscopic examination of the control mice revealed that the SSM layer existed in the innermost surface of the circular muscle layer (Fig. 4a). Compared to the bulk smooth muscle (BSM) cells, the SSM cells had dendric appearance and darker cytoplasm. In addition, in control mice the ICC were observed between the inner circular muscle layer and the outer layer, corresponding to the darker cells detected by light microscopy. These had flat nuclei, long processes, dark cytoplasm and numerous caveolae. They also formed continuous networks and presented close association with the deep muscular plexus. In contrast, in the experimental mice, the SSM cells could not be distinguished from BSM cells (Fig. 4b). The SSM cells lost their complexity and darker cytoplasm. Moreover, some cells with characteristics of ICC were hardly ever observed between the inner circular muscle layer and the outer layer. No remarkable

changes were seen in mucosa, submucosal regions and BSM cells.

Discussion

The present study examined impairment of interstitial cells of Cajal (ICC) in the region of the myenteric plexus in experimental mice. As described in the Results section, immunoreactions for *c-kit* detected in control mice were identical to the localization of ICC in the region of the myenteric plexus (refereed to as ICC-MP). In the experimental mice, the monoclonal ACK2 antibody was used both for immunohistochemistry and for antagonizing *c-kit* function. As shown in Figure 2a-c, the disappearance of *c-kit* immunoreactions indicates the alteration and/or decrease of the *c-kit* tyrosine kinase receptors. Therefore, some cells characterized with thin processes examined in the experimental mice, as shown in Figure 3c-d, have the possibility to be transformed ICC-MP. If so, such changes of ICC-MP would suggest that ACK2-binding sites existed at the surface of ICC-MP. Original structures of ICC were reported for the first time by Cajal[15-16]. Kobayashi *et al.* claimed that the interstitial cells described by Cajal might be an artefactual chimera of glial cell bodies and nerve fibres, therefore the ICC need not necessarily be classified as an independent cell category[17-19].

However, many studies concerning the morphology of ICC have been reported[20-24], and morphological criteria for ICC will be advocated[25-27]. The ICC-MP in control mice in the present study were confirmed to correspond to those criteria. They have been assumed to function as intestinal pacesetters, which generate slow wave activity[25-31]. Electrophysiologically, Hara *et al.* demonstrated that the slow wave activity in the small intestine of mammals was generated by non-neural cells located between the longitudinal and circular muscles[28]. Some slow waves with maximal amplitude were detected at the myenteric border in the intestines[29-30]. It has also been reported that some jejunal strips of cat oscillated no slow waves without ICC-MP[29], and that selective uptake of methylene blue into ICC-MP inhibited the slow wave activity[31]. These findings would confirm that the ICC-MP played an essential role in the generation of slow wave activity. Accordingly, the network formation of ICC-MP appears to be required for conduction of the electrical signals[20]. In the present study, experimental mice presented severe obstruction-like symptoms together with the impairment of ICC-MP, indicating that the dysfunction of the intestinal pacemaker system. Concerning this point, further examinations are needed in conjunction with electrophysiological evidence.

We found the impairment of ICC in the region of the deep muscular plexus, and morphological alterations of the special smooth muscle (SSM) cells in the experimental mice. ICC in the region of the deep muscular plexus (referred to as ICC-DMP) have different characteristics in ultrastructure from that of normal control mice[25-27], though those of the controls presented were well compatible with the ICC criteria. In the present study, no remarkable immunoreactions concerning *c-kit* existed in the inner circular muscle layer, although both ICC-DMP and SSM presented morphological impairment in the experimental mice. Our ultrastructural study did not reveal a direct coupling between ICC-MP and ICC-DMP by cable-like ICC, which interacts between ICC-MP and ICC-DMP. Therefore, the mechanism of simultaneous impairment of both ICC-DMP and SSM remains unclear[27]. ICC-DMP, however, are assumed to play a role in another set of poten-

tial pacemakers[25–28], and electrophysiologically, might cooperate with ICC-MP[30]. Some changes in ICC-DMP would probably occur secondarily after the impairment of ICC-MP by an unknown etiology.

Regarding SSM cells, Gabella reported that the innermost layer of the circular muscle consisted of special dark and small smooth muscle cells, which also contained numerous nerve fibers[32]. Torihashi *et al.* claimed that ICC-DMP was a specialized type of smooth muscle cell[33], while other investigators have also reported morphological resemblance between ICC and smooth muscle cells[23–24]. In the present study, ICC-DMP in the control mice presented a similar ultrastructural appearance to that of SSM. In addition, synchronous impairment of ICC-DMP and SSM in our experimental mice suggested some functions of SSM which were in concert with intestinal pacemaker systems. The ICC-DMP is also suggested to function as mechano-receptors for changes in the tension of intestinal smooth muscles and mediators between nerves and smooth muscle cells[24–26]. In addition, SSM is assumed to function as mechano-receptors for stretching[32]. In the present study, dilatation of the intestines in the experimental mice could be related to the mechano-receptor function of ICC-DMP and SSM. The close association of ICC-DMP with the deep muscular plexus might be suitable for the role of ICC-DMP as mediators in the transmission of signals from nerves to smooth muscles. Numerous histological studies have demonstrated both ICC-DMP and ICC-MP are recognized as pacemaker cells[25–29], but further examinations in combination with both histological and electrophysiological findings are required to clarify the concept of ICC networks as intestinal pacemaker systems.

Pathophysiological findings strongly suggest that the major mechanism of experimental intestinal disease is dysfunction of intestinal movement[11–12]. Accumulation of intestinal contents in the experimental mice suggests the malfunction of intestinal transportion. However, normal intramural plexuses and bulk smooth muscles in the experimental mice suggests the maintenance of their intestinal contractility. As shown in Figure 3a-d, remarkable morphological changes occurred in the ICC system, which had a strong relationship with electrophysiological pacemaker function[25–29].

Some relations between the *c-kit* expression and the intestinal pacemaker system have been reported elsewhere[11–12,34]. Maeda *et al.* reported that intestinal strips of *c-kit* deficient model mice lost electrical rhythm, though no morphological changes in ICC occurred under their experimental conditions[11]. Torihashi *et al.* found morphological alterations of fibroblast-like cells in the intestine of experimental mice which had blocked *c-kit* expression by ACK2 injection[12], but they could not conclude whether such cells were identical to ICC. Moreover, they did not examine ultrastructural changes in SSM layers. Functionally, neither studies[11–12] reported severe malnutrition of the experimental mice, as shown in Figure 1a-c. Huizinga *et al.* investigated some strains of *W*-mutant mice and reported both simultaneous defects of ICC-MP and slow waves in the intestine[34]. Their observations were compatible with our study, but they did not report changes of ICC-DMP in the intestine of *W*-mutant mice. Consequently, the present study describes that impairment in both ICC and SSM induced intestinal disorder of mobility in experimental mice for the first time, although the molecular mechanism of *c-kit* receptor tyrosine kinase on pacemaker function remains unclear. In conclusion, we report an experimental pacemaker dis-

ease model in mouse intestines, which presented impairment of both ICC and SSM by the blockade of *c-kit* receptor function.

ACKNOWLEDGEMENTS

The authors thank Prof. S. Nishikawa and Prof. K. Nishi of Kumamoto University School of Medicine and previous Prof. S. Kobayashi of Nagoya University School of Medicine for their gifts of ACK2, Prof. N. Yanaihara of Shizuoka Prefectural University for providing anti-substance P and anti-VIP antibodies, and Prof. M. Suzuki of Yamanashi Gakuin University and Dr. H. Ohtsuka of Yamanashi Medical University for their technical assistance. The present study was supported in part by Grants-in-Aid No. B2-08457165 to M.A. Fujino from the Japanese Ministry of Education, Science and Culture.

REFERENCES

1) Yarden Y, Kuang WJ, Yang-Feng T, Coussens L, Munemitsu S *et al.*: Human proto-oncogene *c-kit*: a new cell surface receptor tyrosine kinase for unidentified ligand. EMBO J, **6**: 3341–3351, 1987.
2) Qiu F, Ray P, Brown K, Barker PE, Jhanwar S *et al.*: Primary structure of *c-kit*; relationship with the CSF-1/PGDF receptor kinase family: oncogenic activation of v-kit involves deletion of extracellar domain and C terminus. EMBO J, **7**: 1003–1011, 1988.
3) Chabot B, Stephenson DA, Champman VM, Besmer P, Bernstein A *et al.*: The proto-oncogene *c-kit* encoding a transmembrane tyrosine kinase receptor maps to the mouse *W* locus. Nature, **335**: 88–89, 1988.
4) Geissler EN, Ryan MA, Housman DE: The dominant white spotting (*W*) locus of the mouse encodes the *c-kit* proto-oncogene. Cell, **55**: 185–192, 1988.
5) Mintz B, Russell ES: Gene-induced embryological modification of primordinal germ cells in the mouse. J Exp Zool, **134**: 207–237, 1957.
6) Nocka K, Majumder S, Chabot B, Ray P, Cervone M *et al.*: Expression of *c-kit* gene products in known cellular targets of *W* mutations in normal and *W* mutant mice-evidence for an impaired *c-kit* kinase in mutant mice. Genes Devel, **3**: 816–826, 1989.
7) Manova K, Nocha K, Besmer P, Bachrarova RF: Gonadal expression of *c-kit* encoded at the *W* locus of the mouse. Development, **110**: 1057–1069, 1990.
8) Orr-Urteger A, Avivi A, Zimmer Y, Givol D, Yarden Y *et al.*: Developmental expression of *c-kit*, a proto-oncogene encoded by the *W* locus. Development, **109**: 911–923, 1990.
9) Nishikawa S, Kusakabe M, Yoshinaga K, Ogawa M, Hayashi S *et al.*: In utero manipulation of coat formation by a monoclonal anti-*c-kit* antibody: two distinct waves of *c-kit*-dependency during melanocyte development. EMBO J, **10**: 2111–2119, 1991.
10) Ogawa M, Matsuzaki Y, Nishikawa S, Hayashi S, Kunisada T *et al.*: Expression and function of *c-kit* in hemopoietic progenitor cells. J Exp Med, **174**: 63–71, 1991.
11) Maeda H, Yamagata A, Nishikawa S, Yoshinaga K, Kobayashi S *et al.*: Requirement of *c-kit* development of intestinal pacemaker system. Development, **116**: 369-375, 1992.
12) Torihashi S, Ward SM, Nishikawa S, Nishi K, Kobayashi S *et al.*: *c-kit* dependent development of interstitial cells and elecrtical activity in the murine gastrointestinal tract. Cell Tiss Res, **280**: 97–111, 1995.
13) Champy C: Granules et substances reduisant de l'iodure d'osmium. J Anat Physiol Paris, **49**: 323–343, 1913.
14) Maillet M: Modification de la technique de Champy au tetroxyde d'osmium-iodure du potassium. C R Sénc Biol, **53**: 939–940, 1959.
15) Cajal SR: Sobre la red nerviosa ganglionar de las vellosidades intestinales. Gaceta Med Catal, **12**: 614–616, 1889.
16) Cajal SR: Sur les ganglions et plexus nerveux de l'intestin. C R Soc Biol Paris, **5**: 217–223, 1893.
17) Endo Y, Endo T and Kobayashi S: Electron microscopic study on S-100 protein immunoreactive cells in the guinea-pig duodenum, with special reference to the interstitial cells of Cajal. Neurosci Lett, **79**: 272–276, 1987.
18) Kobayashi S, Suzuki M, Endo T, Endo Y, Uchida T: Framework of the enteric nerve plexuses: an immunocytochemical study in the guinea-pig jejunum using an antiserum to S-100 protein. Arch Histol Jpn **49**: 159–188, 1986.
19) Kobayashi S, Furness JB, Smith TK, Pompolo S: Histological identification of the interstitial cells

of Cajal in the guinea-pig small intestine. Arch Histol Cytol, **52**: 267–286, 1989.

20) Komuro T: Three-dimensional observation of the fibroblast-like cells associated with the rat myenteric plexus, with special reference to the interstitial cells of Cajal. Cell Tiss Res, **255**: 343–351, 1989.
21) Zhou DS, Komuro T: Interstitial cells associated with the deep muscular plexus of the guinea-pig small intestine, with special reference to the interstitial cells of Cajal. Cell Tiss Res, **268**: 205–216, 1992.
22) Rumessen JJ, Thuneberg L: Plexus musclaris profundus and associated interstitial cells. I. Light microscopic studies of mouse small intestine. Anat Rec, **203**: 115–127, 1982.
23) Rumessen JJ, Thuneberg L: Interstitial cells of Cajal in human small intestine. Ultrastructural identification and organization between the main smooth muscle layers. Gastroenterology, **100**: 1417–1431, 1991.
24) Rumessen JJ, Mikkelsen HB, Thuneberg L: Ultrastructure of interstitial cells of Cajal associated with deep muscular plexus of human small intestine. Gastroenterology, **102**: 56–68, 1992.
25) Thuneberg L: Interstitial cells of Cajal: interstitial pacemaker cells? Adv Anat Embryol Cell Biol, **71**: 1–130, 1982.
26) Thuneberg L: Interstitial cells of Cajal. In: Wood JD, Bethesda MD eds. Handbook of Physiology. I. Am Physiol Soci, Washington DC. 349–386, 1988.
27) Daniel EE, Berezin I: Interstitial cells of Cajal: are they major players in control of gastrointestinal motility? J Gastroent Motil, **4**: 1–24, 1992.
28) Hara Y, Kubota M, Szurszewski JH: Electrophysiology of smooth muscle of the small intestine of some mammals. J Physiol, **372**: 501–520, 1986.
29) Suzuki N, Prosser CL, Dahms V: Boundary cells between longitudinal and circular layers: essential for electrical slow waves in cat intestine. Am J Physiol, **250**: G287–G294, 1986.
30) Smith TK, Reed JB, Sanders KM: Origin and propagation of electrical slow waves in circular muscle of canine proximal colon. Am J Physiol, **252**: C215–C224, 1987.
31) Thuneberg L, Johansen V, Rumessen JJ: Interstitial cells of Cajal: selective uptake of methylene blue inhibits slow wave activity. In: Roman C ed. Gastrointestinal Motility. MTP, Lanchester. 495–502, 1984.
32) Gabella G: Special muscle cells and their innervation in the mammalian small intestine. Cell Tiss Res, **153**: 63–77, 1974.
33) Torihashi S, Kobayashi S, Gerthoffer WT, Sanders KM: Some interstitial cells in canine small intestine are specialized smooth muscle cells. Am J Physiol, **265**: G638–645, 1993.
34) Huizinga JD, Thuneberg L, Klüpel M, Malysz J, Mikkelesen HB *et al.*: *W/kit* gene required for interstitial cells of Cajal and for intestinal pacemaker activity. Nature, **373**: 347-349, 1995.